INFLUENCE OF CHROMIUM NITRIDE CERAMIC LAYERS THICKNESSES DEVELOPED ONTO 310 H STAINLESS STEEL ON THE CORROSION RESISTANCE

Aurelia Elena TUDOSE[1,2], Florentina GOLGOVICI[3], Ioana DEMETRESCU[4,5], Manuela FULGER[2], Alexandru ANGHEL[6], Oana BRINCOVEANU[7]

Chromium nitride (CrN) layers of different thicknesses applied on the surface of 310 H stainless steel using the thermionic vacuum arc (TVA) technique were characterized through surface analysis methods (SEM, EDX, GIXRD) and electrochemical tests (potentiodynamic polarization and electrochemical impedance spectroscopy). Higher polarization resistance value of 1.823×10^5 $k\Omega\times cm^2$ obtained in the case of samples coated with a CrN thicker layer indicated that the thicker coatings are more protective and provide better corrosion resistance than thinner ones, a conclusion highlighted by the potentiodynamic polarization tests results.

Keywords: corrosion resistance, CrN coating, TVA, SEM, EDX, GIXRD, EIS

1. Introduction

The austenitic and ferritic stainless steel have been used in nuclear power plants for many years, and the austenitic 304L and 316L grades were frequently selected as the most effective in corrosive environments [1, 2]. Years ago, the corrosion tests were performed under simulated boiling water and primary pressurised water reactor and temperature range was from 70 to 320°C [1]. More recently austenitic stainless steel became interesting as corrosion resistant material for much larger temperature domain and more aggressive environment for the future IV reactor generation [2] and many investigations started for the 310H and

[1] PhD Student, Dept. of General Chemistry, University POLITEHNICA of Bucharest, Romania, e-mail: acirciuvoianu3010@stud.chimie.upb.ro
[2] Researcher, Dept. of Nuclear Materials and Corrosion, RATEN Institute for Nuclear Research, Mioveni, Romania, e-mail: aurelia.tudose@nuclear.ro; manuela.fulger@nuclear.ro
[3] Assoc. Prof., Dept. of General Chemistry, University POLITEHNICA of Bucharest, Romania, e-mail: florentina.golgovici@upb.ro
[4] Prof., Dept. of General Chemistry, University POLITEHNICA of Bucharest, Romania, e-mail: ioana.demetrescu@upb.ro
[5] Academy of Romanian Scientists, Bucharest, Romania, e-mail: ioana.demetrescu@upb.ro
[6] Researcher, Low Plasma Temperature Laboratory, National Institute for Laser, Plasma and Radiation Physics, Magurele, Romania, e-mail: alexandru.anghel@inflpr.ro
[7] Researcher, National Institute for Research and Development in Microtechnologies - IMT Bucharest, Bucharest, Romania, e-mail: oana.brincoveanu24@gmail.com

316L types coated and uncoated [3-6]. Researchers have developed several coated materials for the nuclear energy as a strategy to increase efficiency [7] and reducing costs [8, 9]. The 310 H stainless steel (SS) has been selected as potential structural material for construction of the internal components of a supercritical water - cooled reactor (SCWR) due to its high corrosion resistance. The corrosion resistance is mainly due to the relative high Cr content which forms, on the surface, a protective layer of chromium oxide (Cr_2O_3) [10]. Although this type of steel has high corrosion resistance, when exposed to high temperatures between 450°C and 850°C, this is sensitized and becomes susceptible to intergranular corrosion, due to chromium carbide precipitation at the grain boundaries [11, 12] and chromium depletion near the grain boundaries [13]. Also, the high chromium content in 310 H makes this steel more susceptible to develop secondary phases (e.g sigma phase) under aggressive conditions like supercritical water (550°C, 250 atm) [14].

To improve the performances of this material, thin ceramic or metallic layer can be deposited on surface using various deposition techniques [15].

Ceramic materials are known for their good resistance in corrosive environments and are suggested as suitable reactor materials for supercritical water applications [16]. Among the metal nitrides, chromium nitride (CrN) is the best coating used for high temperature and high-pressure work due to its good properties such as high hardness, high ductility, higher toughness, lower friction coefficient, wear resistance as well as oxidation resistance (begins to oxidize at 700°C) [17-21]. CrN coatings were usually prepared by physical vapor deposition (PVD) techniques. Depending on the deposition techniques and parameters used, the mechanical properties, phase compositions and microstructure of CrN coatings may change. The variation of the nitrogen pressure led to obtain the films varying in composition from mixtures of Cr and Cr_2N, pure Cr_2N through Cr_2N-CrN to pure CrN [22].

The main objective of this paper and its novelty is to obtain by the TVA method and to characterize CrN layers with different thicknesses developed onto 310 H SS. The surfaces of coated samples have been analyzed using techniques as scanning electron microscopy (SEM), energy dispersive X-ray spectroscopy (EDX) and Grazing Incidence X-ray Diffraction (GIXRD). The general corrosion susceptibility of coated samples, respectively the protective character of the CrN ceramic layers have been assessed using electrochemical methods (linear potentiodynamic polarization and electrochemical impedance spectroscopy).

2. Experimental

The 310 H SS alloy was provided by Outokumpu Stainless AB Company (Degerfors, Sweden) in the form of the sheet with a thickness of 2 mm. The chemical composition of this material is presented in Table 1.

Table 1

Chemical composition of 310 H SS (provided by the supplier) [23]

Alloy	Element, [wt., %]								
	C	Si	Mn	P	S	Cr	Ni	N	Fe
310 H	0.063	0.71	1.61	0.016	0.001	24.13	19.03	0.04	54.34

For all experiments, the samples were cut from the 310 H SS sheet in parallelepipedal shape with the dimensions 25 mm x 15 mm (length x width). They were provided with a hole of 3 mm diameter at one end for mounting of the samples on deposition holder. The samples were polished using SiC abrasive paper with increasing grain size up to 600. Then they were degreased in acetone, rinsed with distilled water, and dried with an air stream. Before deposition, the samples were ultrasonicated in an isopropyl alcohol bath for 15 minutes, followed by blowing nitrogen under high pressure.

To obtain the films of CrN by the TVA method, the N_2 gas was injected into Cr plasma. For coating, 1 - 3 mm Cr pellets of 99.99% purity purchased from NEYCO company (Vanves, France) and N_2 gas of 99.9999% purity purchased from SIAD company (Bergamo, Italy) were used. The depositions have been made at the Low Temperature Plasma Laboratory from National Institute for Laser, Plasma and Radiation Physics (NILPRP, Magurele, Romania). The deposition parameters used for obtained CrN coatings of different thicknesses by TVA method are presented in Table 2.

CrN-coated samples of two different thicknesses were used in this study. The thickness estimated based on gravimetric measurements using an analytical quartz balance, were estimated to be around 300 nm for the thinner CrN layer and around 600 nm for thicker CrN deposited layer. All experiments were performed in triplicate.

The scanning electron microscopy (SEM) was used to investigate the surface morphology using a Fei Quanta scanning electron microscope (FEI, Olanda). To identify the elemental composition, an energy dispersive spectrum detector EDX was used.

Table 2

Deposition parameters used for obtained CrN coating by TVA method

	CrN thinner layer/310 H SS	CrN thicker layer/310 H SS
Filament current, I_f, (A)	55	41
Discharge current, I_d, (A)	3.4	3.6
Discharge voltage, U_d, (V)	100	136
Deposition time, (min.)	80	505
Anode-substrate distance, (cm)	27	30
Flow N_2, (sccm)	25	25

The composition and structure of the deposited layers was investigated by Grazing Incidence X-ray Diffraction (GIXRD) method using a X'Pert PRO MPD Diffractometer (PANalytical B. V., Netherlands, Almelo) in a θ–2θ geometry using CuKα radiation (l = 1.5406 Å). The GIXRD patterns were made at a grazing angle of 5º in the 20º-100º range. To set the experimental analysis conditions, the X'Pert Data Collector program was used. The identification of the phase was made by referring to the International Center for Diffraction Data—ICDD (PDF-4+) database.

Electrochemical methods

The corrosion resistance of the 310 H SS samples coated with CrN layers of different thicknesses has been performed by two electrochemical methods: linear potentiodynamic polarization and electrochemical impedance spectroscopy (EIS), described extensively in other work [24]. The electrochemical tests were performed using an electrochemical system PARSTAT 2273 potentiostat/ galvanostat (Princeton Applied Research, AMETEK, OakRidge, USA). The determinations were made using a classical electrochemical cell with three electrodes: a saturated calomel reference electrode (SCE) as reference electrode (RE); a graphite rod counter - electrode (EC) and plate of uncoated and CrN coated 310 H SS sample as working electrode (WE). All the potentials are measured versus a saturated calomel electrode (SCE) (-241 mV). The electrochemical tests were carried out at room temperature (22 ± 2°C) in borate buffer solution (0.05 M boric acid with 0.001 M borax solution) with a pH = 7.7 ÷ 7.8. This solution is chemically inert and did not affect the coating layers features.

Electrochemical impedance spectroscopy tests were performed at open circuit potential by application of 10 mV amplitude ac voltage in the frequency range between 100 kHz and 100 mHz. The impedance data were analyzed using Nyquist and Bode plots. To obtain quantitative data, the experimental EIS results were simulated with equivalent electrical circuits as appropriate models using ZView 2.90 software.

Potentiodynamic plots were recorded by polarizing of all samples at 0.5 mV s^{-1} scan rate in a potential range between –0.250 V vs. OCP and +1.0 V.

3. Results and discussion

3.1. SEM characterization

The coating morphology evolution depending on the thickness is presented in the SEM images from Fig. 1. The SEM images show the morphology of the surfaces of the uncoated and the coated samples analyzed at different magnifications. The deposited layer being very thin, it could not be visualized at lower magnification.

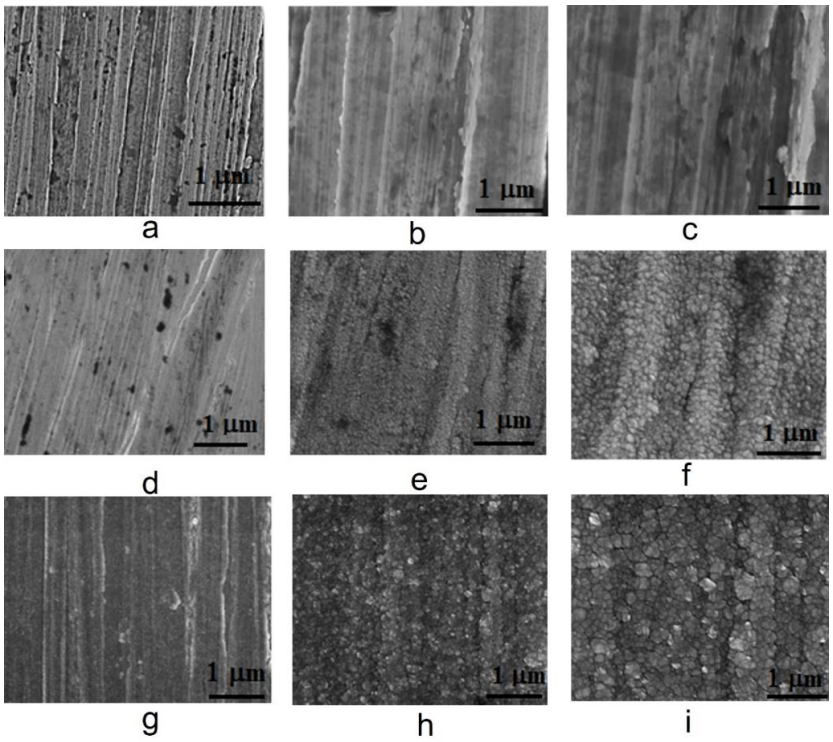

Fig. 1. SEM image of uncoated 310 H SS sample (a-c), 310 H SS sample coated with a thinner CrN layer (d-f) and 310 H SS sample coated with a thicker CrN layer (g-i) at different magnifications

The surface SEM image revealed a granular deposition layer with smaller grains in the case of samples coated with a thinner layer and larger grains in the case of samples coated with a thicker layer. In all cases, the coating layer is uniform, compact and dense, without pores and cracks (Figs.1e and f, Figs. 1h and i). Also, on the surface of the samples, the sanding traces can be observed (this is due to the fact that the samples were polished on abrasive paper up to 600 granulation).

In Table 3 is presented the elemental composition obtained by surface EDX analysis for all three samples. The surface EDX analysis for the uncoated sample shows that the elements corresponding to the substrate (Cr, Fe and Ni) are present. An increase in the chromium and nitrogen contents (up to 38.91%, respectively 16.01%) and a decrease in iron and nickel contents (up to 36.31%, respectively 12.38%) can be observed on the coated samples. The increase of the Cr and N amount proves the formation of a CrN layer on the 310 H stainless steel surface.

Table 3

Elemental composition of uncoated and 310 H SS samples coated with CrN layers of different thicknesses obtained by EDX analysis

Sample type	Elemental composition, (%)								
	C	N	O	Si	Cr	Mn	Fe	Ni	S
uncoated 310 H SS	0.15	-	-	2.52	24.38	-	53.95	18.9	0.09
CrN thinner layer/310 H SS	0.33	6.99	1.64	1.40	30.46	1.41	37.00	14.49	0.06
CrN thicker layer/310 H SS	-	16.01	1.24	0.28	38.91	1.08	36.31	12.38	-

The fact that a CrN layer has been deposited on the surface of the 310 H SS samples is also evident from the in-line EDX analysis presented in Fig. 2.

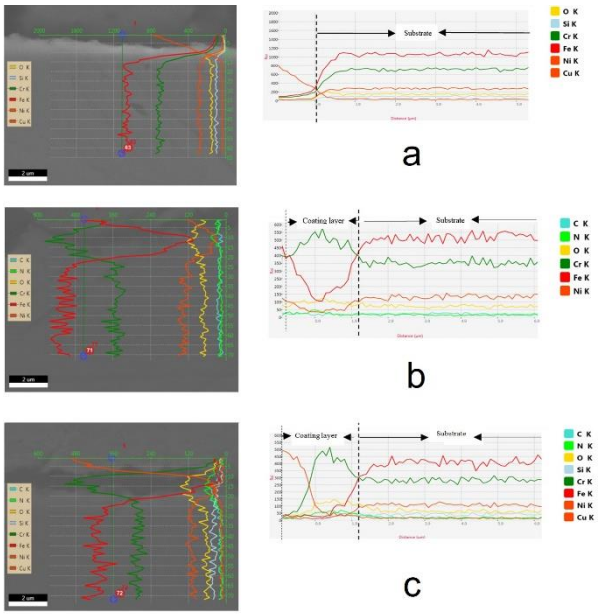

Fig. 2. In-line EDX analysis of uncoated 310 H SS sample (a), sample coated with a thinner CrN layer (b) and sample coated with a thicker CrN layer (c)

This in-line composition determination starts from the coated area and passes through the substrate. An increase in the chromium and nitrogen content (dark green and phosphorescent green lines) and a decrease in the iron and nickel contents (red and brown lines) can be observed in the coated area. In the area of the 310 H substrate can be seen the presence of a large amount of iron (red line).

3.2. GIXRD analysis

Grazing Incidence X-ray Diffraction (GIXRD) was used to examine the phase composition and structure of coated and uncoated studied samples. The GIXRD patterns of the uncoated 310 H SS sample and coated with CrN layers of different thicknesses are shown in Fig. 3. As can be seen, the XRD patterns of

310H stainless steel are represented by a black line and is similar with the literature [25], the peaks correspond with XRD pattern of austenite. The presence of CrN as layer deposited on alloy surface, with a (200) preferred orientation is revealed in the case of two thicknesses CrN coated steel [6].

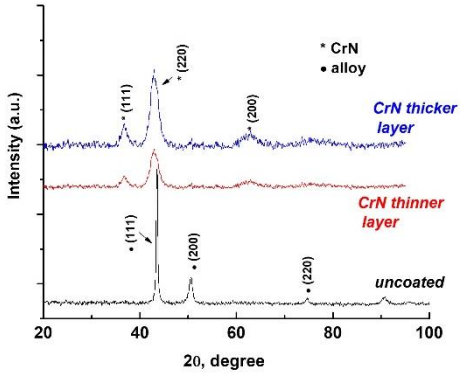

Fig. 3. GIXRD patterns of the CrN coated 310 H SS sample

3.3. Potentiodynamic Polarization Tests

The potentiodynamic polarization plots (shown in Fig. 4) of the sample before and after coating in order to observe the CrN coated 310 H alloy behavior.

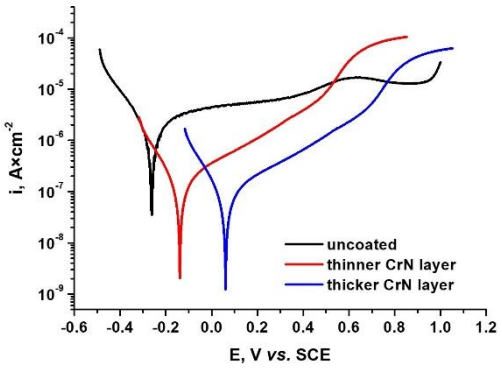

Fig. 4. Potentiodynamic polarization plots for uncoated 310 H SS sample and coated with CrN layers of different thicknesses

From polarization plots (Fig. 4), the electrochemical parameters were calculated using two methods: the Tafel slopes and polarization resistance. The values obtained for the corrosion potential (E_{corr}), the corrosion rate (v_{corr}), the corrosion current density (i_{corr}) and polarization resistance (R_p) are shown in Table 4. Based on the electrochemical parameters obtained, the protective efficiency P_i (%) and the porosity P (%) of the CrN coating have been evaluated quantitatively using Equations (1) and (2), respectively [26]. The polarization resistance method is one of the methods that can be used for assessing the porosity [27, 28]. Porosity

is an important parameter for defect densities evaluation [6, 29], a low porosity value indicating a high protective efficiency.

Table 4

Electrochemical parameters for 310 H SS with and without CrN coating

Sample type	Tafel slopes method		Polarization resistance R_p method			
	E_{corr}, mV	i_{corr}, nA/ cm^2	$R_{p,}$ kΩ×cm^2	i_{corr}, nA/ cm^2	Pi, [%]	P, [%]
uncoated 310 H SS	-256	1030	26	1191	-	-
CrN thinner layer/310 H SS	-140	70.3	372	68.1	93.2	0.4
CrN thicker layer/310 H SS	69	55.4	421	54.7	94.7	0.3

As can be seen from Table 4, the two methods yield a similar value of the electrochemical parameters. The increase of the coating thickness leads to the decrease of the corrosion rate. Therefore, the sample coated with a CrN_x thicker layer are more protective and can provide better corrosion resistance compared to sample coated with a thinner layer or uncoated sample. Also, for this sample the highest protective efficiency (94.7 %) and the lowest porosity (0.3%) values were obtained. Literature data [30-32] showed that the samples with lower corrosion current densities and lower corrosion rates, as well as higher polarization potentials and higher polarization resistances, showed the best coating protective efficiencies, which means a higher ability to prevent corrosion.

3.4. EIS tests

Electrochemical Impedance Spectroscopy (EIS) tests for uncoated and 310 H SS samples coated with CrN layers of different thicknesses have led to the recording of the spectra presented as Nyquist and Bode diagrams (Fig. 5).

The qualitative interpretation of Nyquist (Fig. 5a) and Bode (Fig. 5b) diagrams leads to the conclusion that the samples coated with a CrN thicker layer are more protective and provide better corrosion resistance. This is indicated by slightly higher value of the impedance and the higher maximum phase angle value (-65º). The Bode diagram (Fig. 5b) reveals the presence of a single time constant corresponding to a single semicircle on the Nyquist diagrams (Fig. 5a). As can be seen from the Nyquist diagram (Fig. 5a) for all samples, an open capacitive semicircle was obtained. The diameters of semicircles increase with thickness coating layer increasing, indicating an increase in polarization resistance, which leads to a decrease of the corrosion rate.

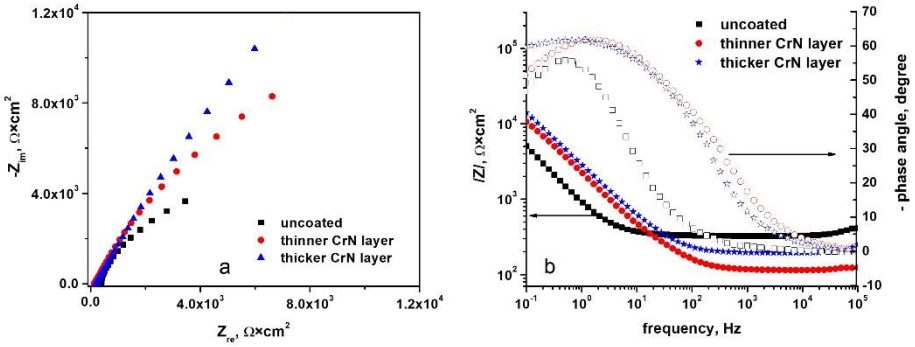

Fig. 5. Nyquist (a) and Bode (b) diagrams for uncoated 310 H SS sample and coated with CrN layers of different thicknesses

The experimental impedance data have been fitted using an equivalent circuit selected with the ZView software. The model for the equivalent electrical circuit proposed to fit the experimental impedance spectra is presented in Fig. 6. The obtained values of equivalent electrical circuit elements are presented in Table 5. Fig. 6 shows, in all cases, that the correlation between experimental data and simulated data is very strong.

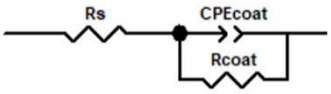

Fig. 6. Model for the equivalent electrical circuit proposed for fitting the experimental impedance spectra

Table 5

The values of equivalent electrical circuit elements for uncoated and CrN_x coated 310 H SS samples*

Sample type	R_s, [Ω×cm^2]	$R_{coat.}$, [Ω×cm^2]	CPE_{coat}-T, [F/ cm^2]	CPE_{coat} - P	Chi-square (χ^2)
uncoated 310 H SS	331.4	8810	2.61×10^{-4}	0.86	1.7×10^{-3}
CrN thinner layer/310 H SS	112.3	111.6	1.15×10^{-4}	0.73	1.4×10^{-4}
CrN thicker layer/310 H SS	195.4	85648	9.07×10^{-5}	0.75	2.1×10^{-4}

* where: R_s is ohmic resistance of the solution; CPE_{coat} is constant phase element for the coating, R_{coat} is resistance of the coating layer.

Applying the Kramers-Kronig transforms, the polarization resistances from the extrapolation of the Nyquist diagrams were determined for all samples (the diameter in Nyquist diagrams is a measure of polarization resistance, R_p). Using the R_p values, the corrosion current density was also calculated, according to the Buttler-Volmer equation. The R_p values obtained from the Nyquist diagram

extrapolation and the corrosion density current calculated from Buttler-Volmer equation are presented in Table 6.

Table 6

R_p values obtained by Nyquist diagram extrapolation and the corrosion density current calculated from Buttler-Volmer equation

Sample type	Polarization resistance from the extrapolation of Nyquist diagrams, ($\Omega \times cm^2$)	i_0 calculated from R_p, ($\mu A / cm^2$)
uncoated 310 H SS	3.381×10^4	3.74×10^{-1}
CrN thinner layer/310 H SS	1.131×10^5	1.12×10^{-1}
CrN thicker layer/310 H SS	1.823×10^5	6.95×10^{-2}

The extrapolation of the Nyquist diagrams (Fig. 5a) shows that the sample coated with a thicker CrN layer has the highest values of polarization resistance (1.823×10^5 $k\Omega \times cm^2$) and the lowest values of corrosion currents (6.95×10^{-2} $\mu A / cm^2$) (Table 6). According to the Buttler-Volmer equation, polarization resistance is inversely proportional to the corrosion current density, so that a higher value of polarization resistance indicates a lower value of the corrosion rate.

6. Conclusions

The corrosion behaviour of 310 H SS samples coated with a CrN layer of different thicknesses by TVA method was described. The surface analysis was investigated morphological and structural by SEM, EDX and GIXRD. The general corrosion susceptibility of coated samples and the protective character of the CrN layers have been assessed by linear potentiodynamic polarization and electrochemical impedance spectroscopy tests. According to the corrosion parameters from the potentiodynamic polarization tests, the 310 H SS sample coated with a thicker CrN layer showed smaller corrosion susceptibility than the sample coated with a thinner CrN layer or the uncoated sample. The EIS analysis with Bode and Nyquist plots have confirmed that the 310 H SS samples coated with a CrN thicker layer are more protective, being in concordance with the polarization tests results.

The current study is assisting the trend towards safer and more secure energy production by concluding the electrochemical and morphological characterisation for the materials of generation IV nuclear reactors.

R E F E R E N C E S

[1] *H. P. Seifert, S. Ritter and H. J. Leber*, „Corrosion fatigue crack growth behaviour of austenitic stainless steels under light water reactor conditions", Corros. Sci., vol. 55, 2012, pp. 61-75.

[2] *A. Stanculescu*, "Worldwide status of advanced reactors (GEN IV) research and technology development. In Encyclopedia of Nuclear Energy", Elsevier: Amsterdam, The Netherlands, 2021, pp. 478–489.
[3] *A. Tudose, I. Demetrescu, F. Golgovici and M. Fulger*, "Oxidation Behaviour of an Austenitic Steel (Fe, Cr and Ni), the 310 H, in a Deaerated Supercritical Water Static System," *Metals*, **vol.** 11, p. 571, 2021.
[4] *V.A. Andrei, C. Radulescu, V. Malinovschi, A. Marin, E. Coaca, M. Mihalache, C.N. Mihailescu, I.D. Dulama, S. Teodorescu and I.A. Bucurica*, "Aluminum Oxide Ceramic Coatings on 316L Austenitic Steel Obtained by Plasma Electrolysis Oxidation Using a Pulsed Unipolar Power Supply", Coatings 2020, **vol.** 10, pp. 318.
[5] *G. S. Was, D. Petti, S. Ukai and S. J. Zinkle*, "Materials for future nuclear energy systems" J. Nucl. Mater. 2019, **vol.** 527, 151837.
[6] *A. Tudose, F. Golgovici, A. Anghel, M. Fulger and I. Demetrescu*, "Corrosion Testing of CrNx-Coated 310 H Stainless Steel under Simulated Supercritical Water Conditions Materials," *Materials*, **vol.** 15, p. 5489, 2022.
[7] *R. Nartita, D. Ionita and I. Demetrescu*, "Sustainable Coatings on Metallic Alloys as a Nowadays Challenge", Sustainability 2021, **vol.** 13, 10217.
[8] *D. Sidelev, M. Syrtanov, S. Ruchkin, A. Pirozhkov and E. Kashkarov*, "Protection of Zr Alloy under High-Temperature 515 Air Oxidation: A Multilayer Coating Approach," *Coatings*, **vol**. 11, p. 227, 2021.
[9] *D. Diniasi, F. Golgovici, A. Anghel, M Fulger, C.C. Surdu-Bob and I. Demetrescu*, "Corrosion Behavior of Chromium Coated Zy-4 Cladding under CANDU Primary Circuit Condition" Coatings 2021, **vol.** 11, no. 11, 1417.
[10] *J. W. D., Callister*, „Materials Science and Engineering an Introduction, 7th Edition, Chapter 11, Jon Wiley & Sons, Inc., 2007.
[11] *Y. Gui, Z. Liang and Q. Zhao*, "Corrosion and carburization behavior of heat-resistant steels in a high-temperature supercritical carbon dioxide environment", Oxid. Met., **vol. 92**, 2019, pp. 123-136.
[12] A. *Yae Kina, S. S. M. Tavares, J. M. Pardal and J. A. Souza*, "Microstructure and intergranular corrosion resistance evaluation of AISI 304 steel for high temperature service", Mater. Charact., **vol. 59**, 2008, pp. 651-655.
[13] *L. Yang, H. Qian and W. Kuang*, "Corrosion Behaviors of Heat-Resisting Alloys in High Temperature Carbon Dioxide", Materials, **vol. 15**, 2022, p. 1331.
[14] *S. S. M. Tavares, V. Moura, V. C. da Costa, M. L. R. Ferreira and J. M. Pardal*, "Microstructural Changes and Corrosion Resistance of AISI 310S Steel Exposed to 600 - 800°C", Short communication, Elsevier, Mater. Charact., **vol. 60**, 2009, pp. 573-578.
[15] *H. Chen, X. Wang and R. Zhang*, "Application and Development Progress of Cr-Based Surface Coatings in Nuclear Fuel Element: I. Selection, Preparation, and Characteristics of Coating Materials", Coatings, **vol. 10**, 2020, p. 808.
[16] *K. Ehrlich, J. Konys and L. Heikinheimo*, "Materials for high performance light water reactors", J. Nucl. Mater., **vol. 327**, 2004, pp. 140-147.
[17] *Z. Wan, T. F. Zang, J. C. Ding, C. - M. Kim, S. - W. Park, Y. Yang, K. - H. Kim and S. - H. Kwon*, "Enhanced Corrosion Resistance of PVD-CrN Coatings by ALD Sealing Layers", Nanoscale Res. Lett., **vol. 12**, 2017, p. 248.
[18] *A. Conde, A. B. Cristóba, G. Fuentes, T. Tate and J. de Damborenea*, "Surface analysis of electrochemically stripped CrN coatings", Surf. Coat. Technol., **vol. 201**, 2006, pp. 3588-3595.
[19] *H. S. Barshilia, N. Selvakumar, B. Deepthi and K. S. Rajam*, "A comparative study of reactive direct current magnetron sputtered CrAlN and CrN coatings", Surf. Coat. Technol., **vol. 201**, 2006, pp. 2193-2201.

[20] *X. S. Wan, S. S. Zhao, Y. Yang, J. Gong and C. Sun*, "Effects of nitrogen pressure and pulse bias voltage on the properties of Cr-N coatings deposited by arc ion plating", Surf. Coat. Technol., **vol. 204**, 2010, pp. 1800-1810.

[21] *A. Ruden, E. Restrepo-Parra, A. U. Paladines and F. Sequeda*, "Corrosion resistance of CrN thin films produced by dc magnetron sputtering", Appl. Surf. Sci., **vol. 270**, 2013, pp. 150-156.

[22] *A. Lippitz and Th. Hu¨bert*, "XPS investigations of chromium nitride thin films", Elsevier, Surface & Coatings Technology, **vol. 200**, 2005, pp. 250-253.

[23] ***Inspection Certificate No. 1293516/18.05.2007-1.4484 - Outokumpu Stainless AB Company.

[24] *M.-E. Voicu and F. Golgovici*, "A biointerface growth at immersion of a biodegradable magnesium alloy in simulated body fluid". U.P.B. Sci. Bull., Series B, **vol**. 82, no. 2, 2020, pp. 57-68.

[25] *M. Dadfar, M.H. Fathi, F. Karimzadeh, M.R. Dadfar and A. Saatchi*, Effect of TIG welding on corrosion behavior of 316L stainless steel, Mater. Lett. **vol.** 61, 2007, pp. 2343–2346.

[26] *M. G. Tsegay, H. G. Gebretinsae and Z. Y. Nuru*, "Structural and optical properties of green synthesized Cr_2O_3 nanoparticle", Mater. Today Proc., **vol. 36**, 2021, pp. 587-590.

[27] *M. Lakatos-Varsányi, F. Falkenberg and I. Olefjord*, "The influence of phosphate on repassivation of 304 stainless steel in neutral chloride solution", Electrochim. Acta, **vol. 43**, 1998, pp. 187-197.

[28] *Y. H. Yoo, J. H. Hong, J. G. Kim, H. Y. Lee and J. G. Han*, "Effect of Si addition to CrN coatings on the corrosion resistance of CrN/stainless steel coating/substrate system in a deaerated 3.5 wt.% NaCl solution", Surf. Coat. Technol., **vol. 201**, 2007, pp. 9518-9523.

[29] *J. A. Olasunkanmi*, "Surface Defects Characterization and Electrochemical Corrosion Studies of TiAlN, TiCN and AlCrN PVD Coatings", Master's Thesis, Tallinn University of Technology, Tallinn, Estonia, 2016.

[30] *L. Zhang, Y. Chen, Y. P. Feng, S. Chen, Q. L. Wan and J. F. Zhu*, "Electrochemical characterization of AlTiN, AlCrN and AlCrSiWN coatings", Int. J. Refract. Met. Hard Mater., vol. **53**, 2015, pp. 68-73.

[31] *Y. H. Yoo, D. P. Le, J. G. Kim, S. K. Kim and P. Van Vinh*, "Corrosion behavior of TiN, TiAlN, TiAlSiN thin films deposited on tool steel in the 3.5 wt. % NaCl solution", Thin Solid Film., vol. **516**, 2008, pp. 3544-3548.

[32] *W. V. K. Grips, H. C. Barshilia, V. E. Selvi and K. S. Rajam*, "Electrochemical behavior of single layer CrN, TiN, TiAlN coatings and nanolayered TiAlN/CrN multilayer coatings prepared by reactive direct current magnetron sputtering", Thin Solid Film, **vol. 514**, 2006, pp. 204-211.